

zonally symmetric numerical modeling of dust storms [2,3] has suggested that this mechanism is ineffective at transporting significant quantities of dust beyond middle latitudes. Recent three-dimensional numerical simulations conducted by us [4], in which the full spectrum of atmospheric eddy motions are present and capable of transporting dust, have shown that the amount of dust transported into polar regions from a southern subtropical source is greatly increased. The eddy transport mechanisms suggested in previous works [5,6] appear to be operating in these simulations.

The apparent preference for dust storm development during northern autumn and winter, when the north seasonal cap is growing, is interpreted as one reason for the retention of a perennial CO₂ residual cap in the south, while in the north all the CO₂ laid down during the winter season sublimates away in the spring. In the north, due to the dust incorporated into the cap during its growth, albedos during springtime are lower than the albedo of the south cap during its spring retreat, which develops during a typically less dusty time of the martian year [7,8]. The less "contaminated" south cap reflects more solar insulation, maintains a lower temperature during spring and summer, and thus is able to retain a cover of CO₂ ice throughout summer. In the north the lower cap albedo results in a larger net radiative flux at the cap surface and the CO₂ cap is unable to survive the summer.

We wish to point out that it is not necessarily the seasonal preference for dust storm development alone that conspires to affect the residual cap and layered terrain variations that are presently seen. Under present orbital characteristics, southern summer solstice occurs close in time to orbital perihelion, producing short "hot" summers and long cold winters in the south. This long cold winter results in a more extensive seasonal CO₂ cap in the south than in the north. The size of the cap can have implications for suspended dust reaching the pole, even in the absence of a global dust storm. Baroclinic waves, which develop due to the large horizontal temperature gradients at middle to high latitudes of the autumn, winter, and spring hemispheres, are probably capable of lifting dust from the surface. This lifted dust can then be carried poleward by these same waves. As the seasonal cap grows, the distance between the location of dust lifting and the pole increases, and thus the dust must be transported a greater distance if it is to become incorporated into the developing cap at polar latitudes, if in fact it can reach those latitudes [5]. Since the southern cap is, at its maximum extent, larger than the northern seasonal cap, the north cap (at polar latitudes) might be more susceptible to dust contamination than the south cap, even without dust storms. In fact, numerical simulations [9] suggest that the magnitude of baroclinic waves is larger in the north than in the south, further increasing the northern hemisphere preference for cap contamination by dust.

We will present model results detailing the mechanisms by which suspended dust is transported into polar latitudes

and quantify polar dust deposition magnitudes as a function of various model assumptions.

References: [1] Pollack et al. (1979) *JGR*, 84, 2929–2945. [2] Haberle et al. (1982) *Icarus*, 50, 322–367. [3] Murphy et al. (1992) *JGR Planets*, submitted. [4] Murphy et al. (1992) in preparation. [5] Pollack J. B. and Toon O. B. (1980) *Icarus*, 50, 259–287. [6] Barnes J. B. (1990) *JGR*, 95, 1381–1400. [7] Colburn et al. (1989) *Icarus*, 79, 159–189. [8] Martin T. Z. (1986) *Icarus*, 66, 2–21. [9] Barnes et al. (1992) *JGR Planets*, submitted.

N 92-87/19816/15 P. 5

NUMERICAL SIMULATIONS OF DRAINAGE FLOWS ON MARS. Thomas R. Parish¹ and Alan D. Howard²,

¹Department of Atmospheric Science, University of Wyoming, Laramie WY 82071, USA, ²Department of Environmental Sciences, University of Virginia, Charlottesville VA 22903, USA.

Introduction: Data collected by the Viking Landers (VL-1, 23°N; VL-2, 48°N) have shown that the meteorology of the near-surface martian environment is analogous to desertlike terrestrial conditions [1]. Geological evidence such as dunes and frost streaks indicate that the surface wind is a potentially important factor in scouring of the martian landscape [2]. In particular, the north polar basin shows erosional features that suggest katabatic wind convergence into broad valleys near the margin of the polar cap. The pattern of katabatic wind drainage off the north polar cap is similar to that observed on Earth over Antarctica [3] or Greenland.

In this paper we will explore the sensitivity of martian drainage flows to variations in terrain slope and diurnal heating using a numerical modeling approach. The model used in this study is a two-dimensional sigma-coordinate primitive equation system [4] that has previously been used for simulations of Antarctic drainage flows. Prognostic equations include the flux forms of the horizontal scalar momentum equations, temperature, and continuity. Explicit parameterization of both longwave (terrestrial) and shortwave (solar) radiation is included [5]. Turbulent transfer of heat and momentum in the martian atmosphere remains uncertain since relevant measurements are essentially nonexistent. Standard terrestrial treatment of the boundary layer fluxes is employed [6–8].

Model Results: *Katabatic wind simulations.* A series of numerical experiments has been conducted that focuses on the relationship between katabatic wind intensity and terrain slope. The model runs are valid for high-latitude (75°), nocturnal conditions similar to midwinter on the north polar cap in which no solar radiation reaches the ground. A horizontal grid consisting of 20 points with a grid spacing of 20 km was used; 15 levels were used in the vertical with higher resolution in the lower atmosphere. The results of five uniform slope runs are presented here. Each model simulation covered

a 24-hr period; terrain slopes were set to 0.0005, 0.001, 0.002, 0.004, and 0.008. In each experiment, the model atmosphere was started from rest to isolate the katabatic wind. An initial lapse rate of $3^{\circ}\text{C km}^{-1}$ was used with a surface temperature of approximately 220 K at the vertical reference level.

In all cases, the katabatic wind reached a quasisteady state within the first 12 hr. The resulting vertical profiles of wind speed and temperature for the five martian katabatic wind simulations after 24 hr are shown in Fig. 1. Curves A-E in this figure correspond to terrain slopes of 0.0005, 0.001, 0.002, 0.004, and 0.008 respectively. The intensity and depth of the katabatic wind (Fig. 1a) appear sensitive to the terrain slope. Note that despite the absence of ambient horizontal pressure gradients in the free atmosphere, a katabatic circulation has developed in the lowest 3 km of the atmosphere after one martian day. It is clear that the radiative flux divergence in the atmosphere acts to influence nearly the entire martian atmosphere. This is considerably different from the Antarctic simulations and is a direct result of the thin martian atmosphere. Even relatively modest values of radiative flux divergence can lead to appreciable temperature change over time and hence the establishment of horizontal pressure gradients.

Figure 1b illustrates the vertical temperature profile in the lowest 3 km for the five cases considered. Pronounced inversion conditions prevail over a deep atmospheric layer. The exponential shapes of the temperature profiles are similar to those seen over the interior of Antarctica although the vertical scale of the martian profiles are much greater than found on Earth. Note that no significant difference is seen in the thermal structure for the five cases despite the fact that the terrain slopes and intensity of the katabatic wind regimes

vary considerably. This again underscores the dominance of the radiation budget in forcing the thermal structure on Mars.

Influence of solar forcing on the martian drainage flows. To test the sensitivity of the martian slope flows to solar forcing, numerical experiments have been conducted in which the full cycle of solar forcing is replicated over sloping terrain. Results for a constant slope of 0.008 at 75° latitude will be described.

Five numerical simulations have been conducted covering the seasonal range of solar declination angles (24° , 12° , 0° , -12° , and -24°); the model equations are integrated for three complete martian days to allow the model to settle into a stable diurnal oscillation. The results presented here are taken from day 2; only minor variations were seen beyond the first diurnal cycle. It is assumed that the polar cap is composed of "dirty" ice with an albedo of 0.50. All simulations start from a rest state. Thus the influence of large-scale pressure gradients in the free atmosphere is neglected. This implies that all atmospheric motions arise due to the long-wave radiative cooling or solar heating of the sloping terrain. No solar insolation is allowed for the first 12 hr of model integration time to allow the drainage flows to become established before model sunrise.

Figure 2 illustrates the diurnal course of the surface temperature, wind speed, and wind direction over the 0.008 slope martian terrain for solar declinations of 24° , 12° , 0° , -12° , and -24° , corresponding to curves A, B, C, D, and E respectively. Here the martian day is divided into 24 martian hours. Note that the Sun never sets during the midsummer period (Fig. 2a, curve A) and never rises for the winter case. The ground temperature (Fig. 2b) undergoes diurnal oscillations of 30 K in summer, with the magnitude of the oscillation decreasing with the approach of the autumn; the diurnal

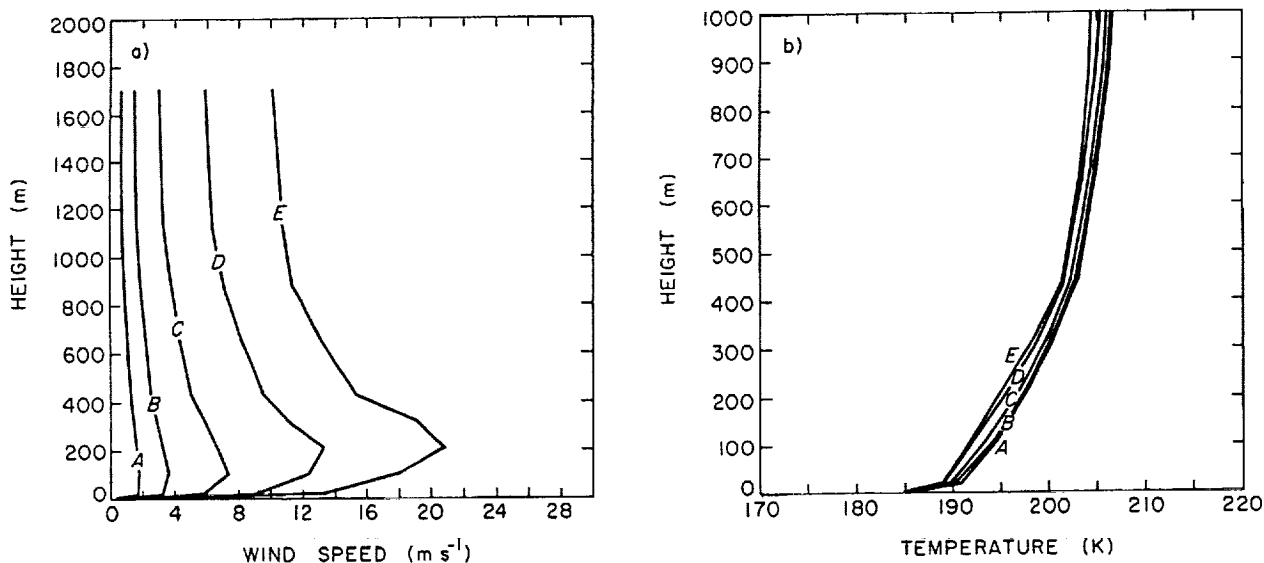


Fig. 1. Vertical profiles of (a) wind speed and (b) temperature in the lowest 3 km after 24-hr integration of constant slope runs.

ground temperature oscillation amounts to 15 K at the equinox. Maximum temperatures appear an hour or so after local noon. Wind speeds at the first sigma level corresponding to approximately 22 m above the surface (Fig. 2c) show marked diurnal trends during summer and equinox periods. Maximum wind speeds occur in the early morning hours coinciding with a minimum in the solar insolation in midsummer or just before sunrise in other simulations. Note that the simulated midsummer katabatic wind maximum of approximately 10.5 ms^{-1} (reached in the early morning hours) is 3 ms^{-1} less than seen for the other cases. This reflects the insolation from the midnight Sun, which retards development of the katabatic wind. Wind directions at the first sigma level throughout the diurnal course for the five numerical simulations are shown in Fig. 2d. The downslope direction is 180° for these simulations. The Coriolis force acts to deflect the

katabatic wind some 30° to the right of the fall line of the terrain for the winter katabatic wind case. The wind directions show surprisingly little variation with time except for the midsummer declination angle of 24° (curve A). Note that upslope flow is modeled during the early afternoon hours of the summer case. The effect of solar insolation appears to retard but not overcome the katabatic forcing in all but the summertime case. This emphasizes the robust nature of the martian katabatic circulation.

Although the most pronounced diurnal changes occur near the surface, significant oscillations can be traced well into the atmosphere. In particular, the strong solar heating of the terrain results in a well-mixed boundary layer that extends upward of 2 km or so by early afternoon. Figure 3 illustrates the vertical structure of temperature and wind speed in the lowest 3 km for the five 0.008 slope experiments at 0200 LT and

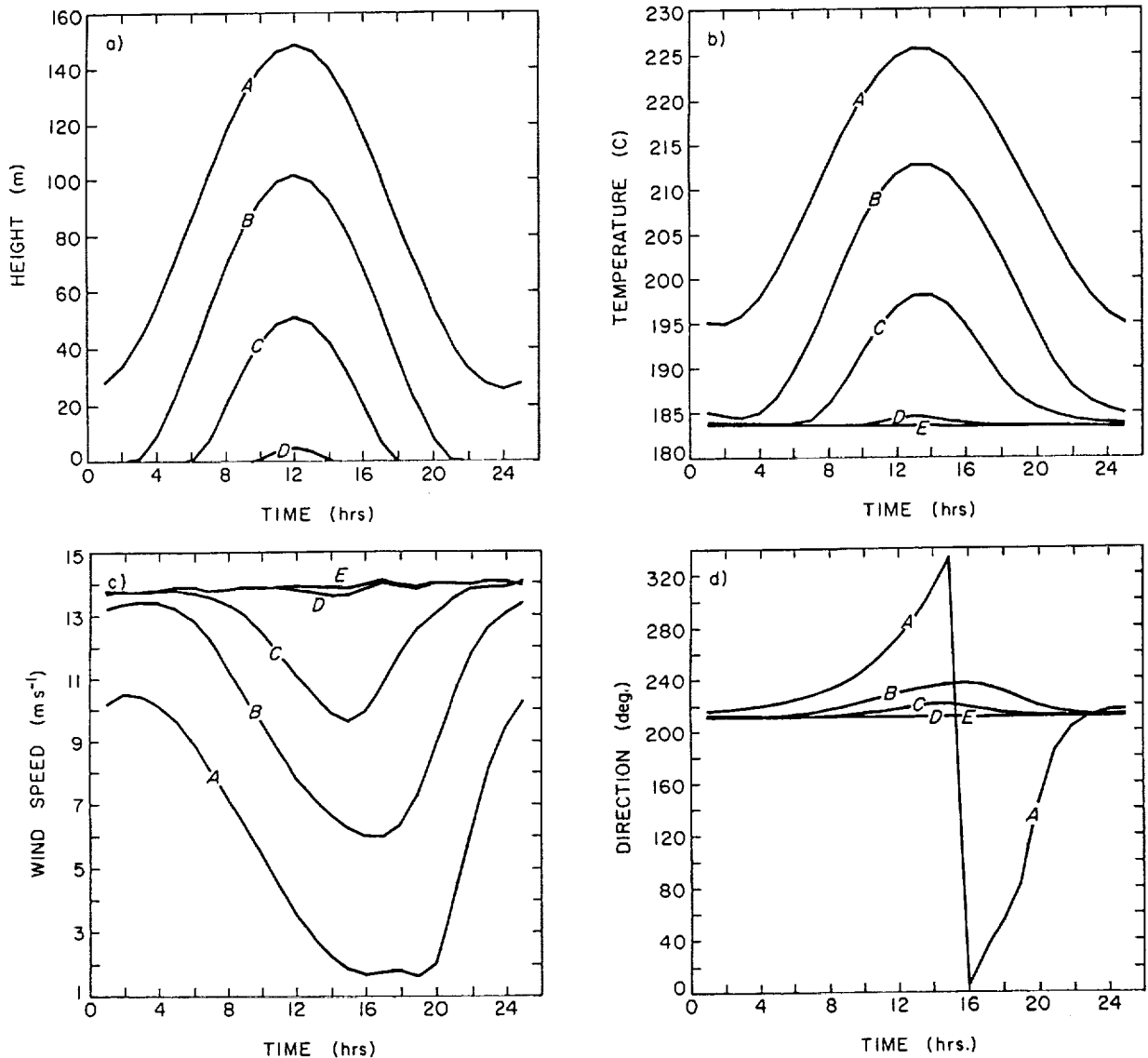


Fig. 2. Diurnal variation of (a) solar insolation reaching the ground, (b) ground temperature, (c) wind speed, and (d) wind direction at the lowest sigma level for the solar cycle simulations over the 0.008 slope.

1200 LT. The temperature profile for the early morning (Fig. 3a) shows an inversion structure for each simulation including the midsummer case (curve A) in which the Sun remains above the horizon for the entire martian day. Although relatively minor diurnal changes are seen above 1 km, seasonal temperature differences are evident. The midsummer thermal structure suggests a near-adiabatic profile above the inversion. The atmospheric stability above the katabatic layer increases as the intensity of solar radiation decreases such that by the equinox, inversion conditions prevail. The thermal structure of the atmosphere at noon (Fig. 3b) indicates adiabatic conditions prevail up to around 2 km during midsummer. The wind speeds (Figs. 3c,d) for the 0.008 slope show well-developed katabatic wind profiles during the early morning hours, although the intensity of the drainage flow is reduced considerably for the midsummer case. Wind speeds

at local noon for the five solar declinations suggest that the katabatic wind regime in the lower atmosphere is considerably reduced by solar radiation during the nonwinter periods. The katabatic wind signature is still present in all but the midsummer case. Little diurnal variation is seen above 1 km.

Summary: Numerical simulations suggest katabatic winds are ubiquitous features of the nocturnal lower boundary layer at high latitudes on Mars. The drainage flows are analogous to those seen over the Antarctic continent, and have comparable scales of wind speeds and depths. Model experiments suggest that longwave radiative cooling is the dominant forcing mechanism for the martian katabatic winds and is responsible for establishing a horizontal pressure gradient in a deep layer over sloping terrain. The intensity of the induced circulation is dependent on the slope of the underlying terrain.

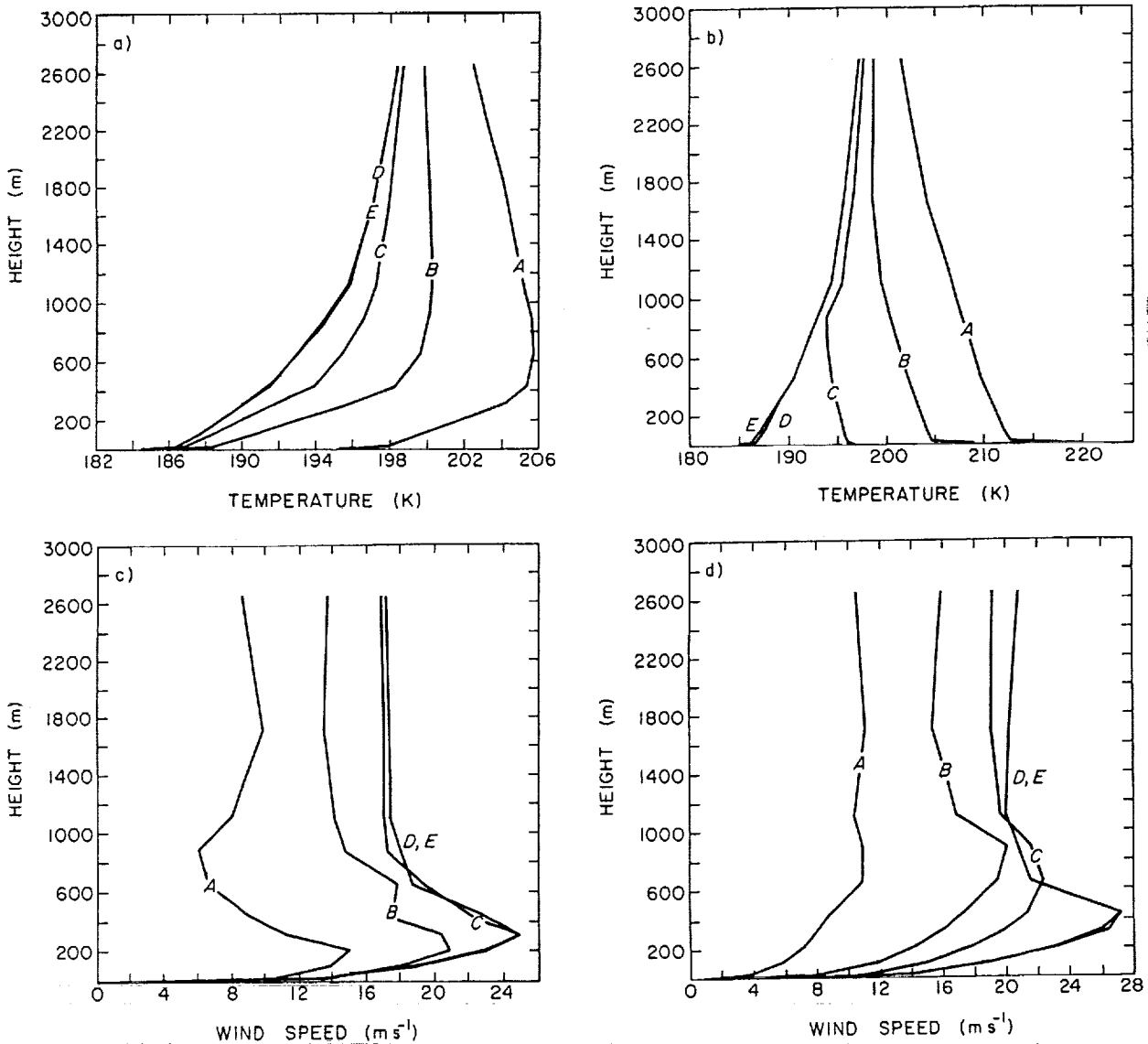


Fig. 3. Vertical profiles of temperature and wind speed in the lowest 3 km over the 0.008 slope at 0200 LT (left) and 1200 LT (right).

Model experiments incorporating the solar cycle show the katabatic wind to be completely suppressed only during the midsummer daytime simulation. The adjustment time for the development of the katabatic wind is quite short; during the early morning hours of midsummer the drainage flows are able to develop. This implies that once the Sun sets, the development of the katabatic wind is very rapid and near-steady conditions prevail in just a few hours.

References: [1] Hess S. L. et al. (1977) *JGR*, 82, 4559-4574. [2] Howard A. D. (1981) *NASA TM-82385*, 333-335. [3] Parish T. R. and Bromwich D. H. (1987) *Nature*, 328, 51-54. [4] Anthes R. A. and Warner T. T. (1978) *Mon. Wea. Rev.*, 106, 1045-1078. [5] Parish T. R. and Waight K. T. (1987) *Mon. Wea. Rev.*, 115, 2214-2226. [6] Brost R. A. and Wyngaard J. C. (1978) *J. Atmos. Sci.*, 35, 1427-1440. [7] Busch N. E. et al. (1976) *J. Appl. Meteor.*, 15, 909-919. [8] Businger J. A. et al. (1971) *J. Atmos. Sci.*, 28, 181-189.

516-N93-1981P-2

ANTARCTIC LAKES (ABOVE AND BENEATH THE ICE SHEET): ANALOGUES FOR MARS. J. W. Rice Jr., Astrogeology Branch, U.S. Geological Survey, Flagstaff AZ 86001, USA.

The perennial ice-covered lakes of the Antarctic are considered to be excellent analogues to lakes that once existed on Mars. Field investigations of ice-covered lakes, paleolakes, and polar beaches have been conducted in the Bunger Hills Oasis, Eastern Antarctica. These studies will also be extended to the Dry Valleys, Western Antarctica, and the Arctic.

Important distinctions have been made between ice-covered and non-ice-covered bodies of water in terms of the geomorphic signatures produced. Field investigations have revealed that the classical lacustrine landforms created by non-ice-covered lakes (spits, bars, berms, cusps, tombolos, and wave-cut platforms) are absent in an ice-covered lake regime. The features mentioned above are the result of the direct coupling of wind and the free water surface. The ice cover acts as a geomorphically protective agent. Therefore, the shores of ice-covered bodies of water are low-energy environments, i.e., poorly sorted, due to restricted or nonexistent wave action.

The most notable landforms produced by ice-covered lakes are ice-shoved ridges. These features form discrete segmented ramparts of boulders and sediments pushed up along the shores of lakes/seas. The shorelines are generally planated with the ramparts defining the inner edge of the shoreline. These ridges usually have a heterogeneous veneer of boulders, pebbles, sand, and gravel mantling an ice core. The ice core normally melts out and leaves behind its mantle of material in the form of irregular discontinuous ridges. The ice core can persist for years if it is sufficiently insulated by its mantle of material.

The ice-shoved features observed in the Bunger Hills Oasis were up to 83 m long, 2 m high, and 4 m wide. Ice-shoved ridges up to 300 m long and 10 m high have been reported [1]. Other unique landforms associated with polar beaches are frost cracks and mounds, patterned ground, pingos, pitted beaches, coastal striated bedrock, and ventifacts. Investigations of ice-covered lakes in Antarctica has also disclosed information that may have important exobiological implications [2-4], namely the discovery of modern, cold-water, blue-green algal stromatolites that are adapted to extremely cold temperatures, fresh-to-saline water, and low light intensities, and the fact that an ice cover acts as both insulating blanket and protective seal for the liquid water located below. The ice cover's "sealing effect" allows the liquid water to retain biologically important gases that are dissolved in the water column.

Several paleolacustrine basins have been located and mapped on Mars [5,6]. The last vestiges of these martian lakes, which eventually froze throughout because the influx of meltwater ceased, are expected to be found at high latitudes. Provided that the ice cover was covered with the appropriate sediment thickness [7], these paleolake remnants would form a massive lens of buried ice. It is proposed that this lacustrine ice lens would be composed of interlayered fluvial/lacustrine sediment and ice. This layering would be created by the influx of sediment brought in by multiple flow episodes from channels located along the periphery of the basin [8-10]. Aeolian deposits would also contribute to the ice cover mantling. More investigative studies and field work will be conducted on these problems.

Sub-Ice-Sheet Lakes: Sub-ice lakes have been discovered [11] under the Antarctic ice sheet using radio echo sounding. These lakes occur in regions of low surface slope, low surface accumulations, and low ice velocity, and occupy bedrock hollows.

The development of Radio Echo Sounding (RES) in the late 1950s was driven by the necessity to measure ice thickness in a rapid, accurate, and continuous manner. RES provides information on electrical properties in ice, enables the study of ice-sheet surface form, thickness, internal structure, dynamics, thermodynamics, and basal conditions and processes [12].

Most of the lakes beneath the Antarctic ice sheet are located near Dome C in Eastern Antarctica [11]. Several very large lakes, up to 8000 km², have been discovered [12]. RES studies do not allow the depth of these lakes to be determined; however, the minimum thickness of a fresh-water layer can be estimated by the skin depth necessary for radio reflection [12]. Some of these lakes may have a minimum depth of 6.5 m.

The sub-ice lakes of Antarctica may have formed more than 5 m.y. ago [11]. This age is based upon deep-sea cores taken in the Ross Sea that indicate that the main Antarctic ice sheet has changed little in size since a retreat some 5 m.y.